Drug Delivery and Translational Research
https://doi.org/10.1007/s13346-024-01688-6

ORIGINAL ARTICLE

An injectable oleogel-based bupivacaine formulation for prolonged non-opioid post-operative analgesia

Susan Wojtalewicz[1] · Jack Shuckra[1] · Keelah Barger[1] · Sierra Erickson[1] · Jonathon Vizmeg[1] · Stefan Niederauer[1] · Andrew Simpson[1] · Jordan Davis[1] · Avital Schauder[2] · Orna Hifi[2] · David Castel[2] · Sigal Meilin[2] · Jayant Agarwal[1] · Caleb Lade[1] · Brett Davis[1]

Accepted: 26 July 2024

Abstract

Opioid-based medications remain the mainstay of post-operative pain management, even though they are associated with a plethora of adverse effects including addiction, nausea, constipation, cognitive impairment, respiratory depression, and accidental death due to overdose. Local anesthetics are effective at controlling the intense pain after surgery but their short duration of effect limits their clinical utility in post-operative pain management. In this manuscript, an optimized injectable oleogel-based formulation of bupivacaine for multi-day post-operative pain management was characterized on the benchtop and assessed in two clinically-relevant porcine post-operative pain models. Benchtop characterization verified the optimized oleogel-based bupivacaine formulation design, demonstrating a homogenous stable oleogel with sufficient injectability due to shear-thinning properties, high drug loading capacity and first-order drug release kinetics over 5 days. In vivo assessment in two pig post-operative pain models demonstrated that the oleogel-based bupivacaine formulation can provide statistically significant multi-day analgesia in two routes of administration: local instillation directly into a surgical site and ultrasound-guided peripheral nerve block injection. Pharmacokinetic assessment of ALX005 found that C_{max} values were not statistically different from the bupivacaine HCl control, with no clinical signs of local anesthetic systemic toxicity observed, when administering up to 2.7 and 8.1 times the control dose of bupivacaine HCl. This study demonstrates the pre-clinical safety and efficacy of an injectable oleogel-based bupivacaine formulation and explores its utility as a single-administration long-acting local anesthetic product for post-operative pain management that can be used in both local and regional anesthetic applications.

Keywords Oleogel · Controlled release · Local anesthetic · Bupivacaine · Regional anesthesia · Injectable

Abbreviations

XRD	X-Ray Diffraction
USP	United States Pharmacopeia
AUC	Area under the curve
MCT oil	Medium-chain triglycerides
DBS	Distress Behavior Scoring
H&E	Hematoxylin and eosin
C_{max}	Maximum plasma concentration
T_{max}	Time to maximum plasma concentration
GRAS	Generally recognized as safe
IID	Inactive ingredients database

✉ Susan Wojtalewicz
susanwojt@gmail.com

[1] Rebel Medicine Inc, 48 S Rio Grande St., Salt Lake City, UT 84101, USA

[2] MD Biosciences, 4 Eli Horovitz St., 7608810 Rehovot, Israel

Introduction

Opioid-based medications remain a mainstay of post-operative pain management, with more than 80% of patients receiving opioid prescriptions after surgery [1]. Unfortunately, up to 10% of these patients may become long-term users, making surgery a critical point at which patients are at increased risk of developing or worsening opioid-use disorders [2, 3]. Opioids have been linked to a variety of negative effects after surgery, including addiction, nausea, vomiting, constipation, cognitive impairment, dizziness, respiratory depression, and higher risk of death due to overdose [4]. Over the period from 1999 to

Published online: 06 August 2024

2020, more than 263,000 people have died in the US from overdoses involving prescription opioids [5]. Opioid-related adverse events also result in higher readmission rates, prolong hospital length of stay by an average of 3 days, and increase the cost of care by an average of $5,000 [6–8]. Altogether, prescription opioids cost the US health care system an estimated $78 billion annually [9]. Despite recent progress, there remains a critical need for more effective, longer acting, non-opioid options for pain relief following surgery [10].

Currently, multimodal approaches consisting of local and/or regional anesthesia, non-opioid systemic medications (e.g., NSAIDs), and opioid-based medications are used to manage post-operative pain with the goal of reducing total opioid exposure to mitigate their negative effects [11, 12]. Systemic medications including NSAIDs and other non-opioid options may be effective for mild to moderate pain, but are often ineffective in controlling the severe pain associated with surgery by themselves [13]. Local anesthetics such as bupivacaine and ropivacaine may be infiltrated in the tissue surrounding a surgical site, however their effective duration is usually limited to several hours, at which point pain returns. Regional blockade of proximal sensory nerves can provide effective post-operative pain relief. However, the effect is again limited by the short half-life of standard local anesthetics [14]. Infusion pumps may be employed but they have drawbacks including poor patient tolerance, misplacement, infection, and high costs. Because of these limitations, an affordable single-application long-acting local anesthetic formulation that can provide safe and effective prolonged analgesia for multiple days has been widely sought after to mitigate the use of opioids after surgery. Decades of research and commercial endeavors have tried to accomplish this elusive goal; however, only a few products have reached regulatory approval and they suffer from technological flaws which have precluded widespread clinical adoption [15–18].

Drug delivery system technological limitations can be attributed as the root cause of the insufficient clinical utility of the current FDA-approved long-acting local anesthetic products. The current products utilize drug delivery approaches consisting of either multivesicular liposomes [19], in situ gelling implants [20, 21], or solid collagen matrix implants [22]. Non-ideal drug release profiles have led to insufficient analgesic efficacy in many of the products. Drug release is either too short (< 1–2 days) or is significantly delayed (slow onset leading to sub-therapeutic drug levels in the early post-operative phase), leading to insufficient analgesic efficacy and duration. Or, if analgesic effect is sufficient through 72 h, there are other technological pitfalls that limit clinical utility, such as the inability to be used in peripheral nerve block indications. The use of alcohols and other organic solvents to reduce the viscosity for injectability and to create in situ gelling formulations prevents some of the current long-acting products to be used perineurally in peripheral nerve block indications. Other products may be too viscous to inject or have a solid implant form-factor, which physically prevents them from being used in regional anesthesia scenarios [23, 24]. Aqueous solutions may lack the viscosity to allow for direct wound instillation, leading to time-consuming administration of over 100 injections in some surgical scenarios to adequately cover the painful tissue [25]. Many of the current options are plagued with high costs of goods that drive up final product price due to their use of costly excipients and complicated manufacturing processes [17]. The ideal long-acting local anesthetic technology for post-operative pain would provide prolonged analgesia for a minimum of 3 days, have minimal local or systemic safety concerns, be capable of being used both locally and as a regional anesthetic, have an easy-to-use form factor suitable for current local instillation and regional anesthetic techniques, and have a low cost of goods to achieve a lower price point.

We hypothesized that an oleogel-based drug delivery system could create a long-acting local anesthetic product with a sum of functional attributes that could address this unmet clinical need. Oleogels are semi-solid systems that are formed by entrapping liquid oil within a three-dimensional network of structuring agents (gelators), typically hard fats or hydrophobic polymers [26]. Their mechanical properties are consistent with hydrogels but their chemical properties are more hydrophobic in nature. Depending on the materials and processing conditions used, oleogels can be formed with a wide range of physiochemical properties [27]. Oleogels initially came to prominence in the food science industry as a potential alternative to saturated fats, however their non-polar characteristics provoked interest in their use as drug delivery systems for lipophilic drugs [28]. Active pharmaceutical ingredients can be loaded into the oil portion via dissolution and result in controlled diffusion-based drug release capable of achieving zero to first-order drug release kinetics [29–31]. Research groups have found that the ideal long-acting local anesthetic has a robust early onset of analgesia followed by a slow tapering effect over 3 days will yield better pain management and shortened recovery time; predictable diffusion-based zero- to first-order drug release kinetics can achieve this [32]. Drug release properties of oleogels can be tuned via engineering the chemical affinity of the liquid oil to a specific active ingredient. Mechanical properties such as shear-thinning and thixotropy can be achieved depending on the materials and processing parameters used, which is useful in injectable depot applications. Oleogels are simple to manufacture and use economical excipients with established biocompatibility and safety in various pharmaceutical applications, including

injectable drug depots [33, 34]. Our group set out to develop an oleogel-based long-acting local anesthetic formulation with the aim of producing a versatile, safe, effective, economical, and widely distributable non-opioid solution for post-operative pain that would be a significant improvement over the currently available options. This manuscript is a continuation of our previous work in which we explored how oleogels can be made with a broad range of physiochemical properties to be used as injectable parenteral drug delivery systems including differences in rheological properties, injectability, shelf-life stability, thermal stability, and controlled-released tunability [33].

In this manuscript, we characterized a single, novel, and optimized oleogel formulation of bupivacaine (ALX005) on the benchtop and then evaluated it in validated pig post-operative pain models to demonstrate its safety and efficacy in two clinically-relevant routes of administration: 1) incisional wound model with local instillation of the oleogel [35], and 2) incisional wound model with an ultrasound-guided sciatic nerve block administration of the oleogel [36]. All excipients of the ALX005 formulation are generally recognized as safe (GRAS) and are listed on the FDA's Inactive Ingredient Database (IID). This study is a continuation of our previous work where we systematically studied oleogel-based local anesthetic delivery systems made with various oil and hard fat gelators for material analytical characterization, mechanical properties, drug release properties, stability, and pain control when compared to bupivacaine HCl and commercially available liposomal bupivacaine in a rat model [33].

Materials and methods

Materials

Bupivacaine freebase (Nortec Quimica, Brazil), medium-chain triglycerides (IOI Oleochemical, Germany), castor oil (Spectrum, USA), and tristearin (IOI Oleo chemical, Germany) were used in oleogel formulation. Oleogel was formulated in 3 mL glass syringes (Hylok, BD, USA). Off the shelf bupivacaine HCl at 0.5% (w/v) (Marcaine, Hospira, USA) was purchased as a control in the animal models.

Oleogel fabrication

A 50:50 (w/w) ratio of medium chain triglyceride oil and castor oil was heated in a beaker to 80℃ using a hotplate with a stir-bar. Bupivacaine freebase was then added at 3% or 6% (w/v) (drug/oil) to the oil mixture. Once dissolved, tristearin was added at 4% (w/v) (tristearin/oil). The solution was allowed to stir until the formulation became clear, approximately 10 min for 100 mL batch. Upon solubilization, the formulation was syringed into 3 mL glass syringes, sealed, and quenched in an ice-bath for 2 h.

Determination of drug loading

Drug loading of ALX005 oleogel was confirmed using reverse phase liquid chromatography (Vanquish UHPLC, Thermo-Fisher, USA). The drug was extracted from 50 mg of the oleogel ($n=2$) with a liquid–liquid extraction of 5 mL of 1% trifluoroacetic acid in water and 5 mL of n-hexane. The aqueous layer was isolated and 5 µL injected into the liquid chromatography system. Where, a mobile phase of acetonitrile and buffer (65:35) was used through a C18, 120 Å, 4.6 × 250 mm, 5 µm column (Acclaim 120, Thermo-Scientific, USA) held at 25 °C. Flow rate was set to 2 mL/min and detector analysis was performed at a wavelength of 210 nm.

In vitro characterization of oleogel

Microscopic imaging

Light microscopy image of ALX005 was obtained using a Keyence VHX-5000 lens with a 54-megapixel complementary metal-oxide semiconductor (CMOS) camera attached to it. Zoom was set to 5000x.

X-Ray diffraction

Diffraction patterns of crystalline structure of ALX005 oleogel, bupivacaine free-base powder, and tristearin powder were recorded on a D2 Phaser (Bruker, USA). Where, approximately 1.5 g of the material was gently placed into the machine. Measurements were performed from 5–50° (2θ) with a copper anode (Cu-Kα radiation, $\lambda = 1.54$ Å) using a detector (LYNXEYE, Bruker, USA).

Differential scanning calorimetry

The thermal profile of bupivacaine, tristearin and ALX005 was determined using differential scanning calorimetry (DSC) (3500 NETZSCH, Selb, Germany). Where, approximately 25 mg of sample was loaded into standard aluminum crucibles (25 µL) with a center pierced lid at room temperature. With a scanning rate of 5 °C/min, the oleogel was heated from 0 °C to 120 °C, isothermally held for 2 min, and then subsequently cooled to 0 °C at the same rate. Peak temperatures were determined using the NETZSCH Proteus software (NETZSCH, Selb, Germany).

Viscosity

A rheometer (HAAKE Mars 60, Thermo-Fisher) was used to measure the viscosity and linear elastic region of ALX005. Using a 35 mm parallel plate set up with a 1 mm gap, approximately 1.5 mL of the ALX005 oleogel was injected through a 1-inch 18G needle onto the rheometer plate for analysis. To obtain viscosity curves, a controlled rate rotational ramp test was conducted five-fold, at 20 °C and at 37 °C ($n = 5$), between shear rates of 0.1 – 470 s^{-1}.

Applied force during injection

The force required during injection was quantified using a dual column mechanical tester with a 1kN load cell attached (Instron, USA). The method used a previously described protocol for quantification of injectability [37, 38]. The set up included the oleogel-filled 3 mL glass syringe (Hylok, BD, USA) fixed by a free-standing polyvinyl chloride pipe where the barrel of syringe can fit inside the pipe but the syringe's flange rest on the sides of it. Each syringe had a 15-inch-long catheter with a 1 mm inner diameter attached to it (TrueCare Biomedix, India). Experimental groups varied needle gauge beginning with no needle (none), or a 4-inch 18G, 20G or 21G, needle attached ($n = 4$). Each syringe was compressed 25 mm by the load cell at the rate of 1 mm•s^{-1} [37, 39]. Results were analyzed at the "steady-state" force which was defined as the average force the formulation exhibits once it has surpassed the break-free forces required to move the plunger and once formulation flow begins.

Oil binding capacity

The ability for ALX005 to retain oil was quantified using oil binding capacity percentage (OBC%) [40]. Where, six ($n = 6$) pre-weighed 2 mL centrifuge tubes were filled with 0.50 g of the oleogel using the 3 mL syringes with a 1-inch-long 18G needle. Tubes were centrifuged (Sorvall Legend Micro 21, ThermoFisher, 63505 Langenselbold, Germany) at 15,000 RCF for 10 min. The outstanding oil from the oleogel was aspirated from the tube and discarded. The tube and remaining formulation were then weighed. The oil binding capacity (OBC%) was calculated as percent using Eq. 1.

$$OBC\% = \frac{((tube\ weight + 0.50g) - (weight\ after\ aspiration))}{0.5g} * 100. \quad (1)$$

Drug release testing and mathematical modeling

The dissolution of bupivacaine free base from ALX005 was assessed using a USP rotating basket apparatus. The baskets were set to a rotation speed of 50 revolutions per minute and immersed in 500 mL of 1 × phosphate-buffered saline solution (1xPBS) with a pH of 6.5 maintained at 37 °C. A minimum volume of 500 mL was chosen to ensure that in the case of drug dumping, the sink concentration would remain at less than half the solubility limit [41]. The pH of the sink was adjusted to further increase the solubility limit and model infinite sink conditions required for proper assessment of drug release. ALX005 was tested in three separate groups: 2.7% (w/v) (drug/oleogel) at a volume of 1.25 mL, 5.4% (w/v) at a volume of 1.25 mL, and 2.7% (w/v) at a volume of 2.5 mL. Dissolution medium samples (1 mL) were collected at predetermined time points. The samples were analyzed using ultraviolet spectrophotometry (Genesys 50, Thermo Scientific, USA) at a wavelength of 272 nm using the second derivative noise reduction method [42, 43]. At completion of release test, Hixson and Crowell's modified version of the Noyes-Whitney first-order mathematical equation was chosen to quantify and model release characteristics;

$$M_{Cumulative} = M_{Depot}\left(1 - e^{-rt}\right) + b \quad (2)$$

where, $M_{Cumulative}$ indicates the cumulative drug mass milligrams released at each timepoint, M_{Depot} indicates the cumulative drug mass milligrams that is sustained release, t is time in hours, r represents the first order kinetic constant (milligram per hour), and b is burst release in milligrams of drug from the system [44].

In vivo pig post-operative pain models

ALX005 at 5.4% (w/v) was compared to one of the clinical standard local anesthetics, 0.5% (w/v) bupivacaine HCl, in two separate post-operative pain assessment pig models: an incisional model using local treatment and an incision model using nerve block treatment methodology. Both utilized young Naïve Danish Landrace × Large White cross-bred male pigs weighing 11–13 kg. All animals were allowed 5 days of habituation and acclimation, in which they would get accustomed to the facilities as well as the researchers coming in and out of their pens each day. All subsequent tests were performed by these same researchers in accordance with study approval by the Committee for Ethical Conduct in the Care and Use of Laboratory Animals. For injection of treatment groups and incision application, animals were anesthetized by 3.5–5% isoflurane & oxygen mixture at 2–3 L/min for approximately 20 min. Antibiotics, 10% Marbocyl was given during the procedure and 3% Syntomicine was applied to the incisions after closure. Note that each surgery was performed twice, once on the 1st day of the study (left side) and once on the 8th day of the study (right side). The first surgery was followed by efficacy metric von Frey (Methods Section: Animal Model Metrics - Von Frey measurement of mechanical hyperalgesia), and

behavioral metrics including behavior scoring and approach time (Methods Section: Animal model metrics - Distress behavior scoring and Time to approach test, respectively). The second surgery is followed by pharmacokinetics where 3 mL of blood is drawn from the vena cava at pre-determined timepoints (Methods Section: Animal model metrics - Pharmacokinetics). Because the pharmacokinetic arm of this study is stressful to the animals, it was performed after a second, separate, surgery to ensure the efficacy and behavior metrics were not influenced. Note this second surgery served as the 7-day timepoint for histology. At the 15th day of each study the animals were sacrificed and both sites (left and right side; 15-day and 7-day wounds respectively) of treatment application harvested for histological analysis.

Incisional post-operative pain model

The Incisional Post-operative Pain Model followed a previously developed protocol [45]. Where, a 7 cm incision was made in the lower lumbar region, parallel and 3 cm lateral to the spine, creating a wound through both the fascia and the muscle retraction. Next, one of three treatment groups (bupivacaine HCl [5 mL; 25 mg of bupivacaine], ALX005 low [1.88 mL; 102 mg of bupivacaine] or ALX005 high [3.75 mL; 203 mg of bupivacaine]) was injected into the wound space and sutured with a 3–0 silk thread.

Sciatic nerve block post-operative pain model

The Sciatic Nerve Block Post-operative Pain Model also followed a previously developed protocol [36]. Using ultrasound guided standard nerve block techniques, one of three treatment groups (bupivacaine HCl [5 mL; 25 mg of bupivacaine], ALX005 low [1.25 mL; 68 mg of bupivacaine] or ALX005 high [2 mL; 108 mg of bupivacaine]) was injected through a 22 G facet tip needle (Uniplex Nanoline, Pajunk, Germany) perineurally, into the fascial plane, of the sciatic nerve. After the injection was complete, a 5 cm incision for von Frey assessment (Methods Section In vivo pig post-operative pain model - Incisional post-operative pain model) was created on the front of the hind limb, distal to the injection site, and sutured with a 3–0 silk thread.

Animal model metrics

Von Frey measurement of mechanical hyperalgesia

Post-operative pain was assessed using the von Frey technique [36, 45–47]. Von Frey filaments (Aesthesio, Ugo Basile, Italy) were applied 0.5 cm from the incision at pre-determined timepoints. Each filament diameter is associated with an applied force as described in Table 1, where the minimum possible applied force was 0.001 g and the maximum applied force was 60 g. Withdrawal reaction was defined as the animal moving away from the stimulus, twisting the trunk or lifting of the leg. Prior to surgery, each animal had a response of greater than or equal to 26 g for the low back incisional model and greater than 15 g for the hind leg incisional model, or it was excluded from the study. After surgery, the incisional area becomes sensitive to mechanical stimulus. The duration of effect for each treatment group (bupivacaine HCl, ALX005 high, and ALX005 low) can be measured using this technique over time [36, 45]. Heavier filaments (1–60 g) were used in the low back incisional model compared to the leg incision model (0.001–15.0 g) due to thicker and less sensitive skin on the lower back as compared to the leg. Area under the curve (AUC) was calculated in GraphPad Prism 10.0.2, which utilizes trapezoidal rule integration, for each individual animal and analyzed by treatment group. Baseline was defined as the 1 g and all peaks above this threshold were summed. Notation defines which timepoints the integral was performed between, e.g., $AUC_{0\text{-}72}$ is defined by integration from 0 to the 72-h timepoint.

Distress behavior scoring

Following operation, the animals were observed for non-evoked, resting pain, using Distress Behavior Scoring (DBS) [45, 48]. DBS utilized a score system of 0 (normal)

Table 1 Filaments used in von Frey experiments. Shaded indicates the filaments used in each respective model

Applied Force (g)	0.001	0.02	0.04	0.07	0.16	0.40	0.60	1.0	1.40	2.0	4.0	6.0	8.0	10.0	15.0	26.0	60.0
Fil. Size	1.65	2.36	2.44	2.83	3.22	3.61	3.84	4.08	4.17	4.31	4.56	4.74	4.93	5.07	5.18	5.46	5.88
Incision Model																	
Nerve Block Model																	

and 1 (distressed) in seven different categories including the ability to stand, the ability to walk, not protecting the incision, not moving away when approached, not showing restlessness, not isolating, and vocalizing normally. A score of 7 indicated distressed behavior observed in all categories while a score of 0 represents normal behavior in all categories. Assessment was not performed in a particular order; behaviors were recorded as exhibited by the animal. The DBS test lasted approximately 3 min per animal.

Time to approach test

In the incisional model only, the approach time of each of the animals was monitored at pre-determined timepoints to measure the non-evoked pain-related anxiety or depression-like reactivity [45, 48]. The normal behavior of pigs is to move away when someone enters their pen and then to slowly approach the researcher as they become familiar [49]. The time for the animals to approach the intruder indicates the level of the animal's discomfort. After habituation, the day before surgery, all animals included in the study had an approach time of 0 s, implying immediate approach to the researcher. Following surgery, approach time increased again with the level of animal's discomfort from surgery and varied with treatment. In other words, the more effective and comfortable the treatment is suggestive of less pain and discomfort the animals feels and leads to faster approach times.

Pharmacokinetics

At pre-determined timepoints post-injection, 3 mL of blood sample was drawn from the vena cava to a K_3 EDTA vacutainer, gently agitated, and immediately placed on ice. Within 30 min of collection, the samples were centrifuged (3500 RPM) for 10 min at 4 °C. The entire resultant plasma was gently separated using a pipette and transferred into aliquots of approximately 300 µL. The aliquots are then stored upright at -80 °C until bioanalytical evaluation for bupivacaine concentration. For analysis, the samples were thawed and injected through an HPLC (LC-20AD, Shimadzu, Japan) with a C8 2.6 µm, 4.6 × 50 mm, column (Kinetec, Phenomenex, USA). The protocol utilized a 0.1% formic acid in water and 0.1% formic acid in acetonitrile mobile phases with a 0.8 mL/min flow rate and a retention time of 1.28 min. This method was performed on 3 animals from each treatment ($N = 3$/group). Area under the curve (AUC) were calculated in GraphPad Prism 10.0.2, which utilizes trapezoidal rule integration, for each individual animal and analyzed by treatment group. Baseline was defined as the 0.01 ng/mL and all peaks above this threshold were summed. Note AUC_{inf} is defined by integration from 0 to the end of the test which was 120 h.

Histological assessment

In the incisional model, the wound in the lower lumbar region, parallel and 3 cm lateral to the spine, was harvested 5 mm thick. It was then cut perpendicularly in the middle and paraffin embedded such that the center cross section of the wound could be studied. The tissue was sectioned, stained with hematoxylin and eosin (H&E), and imaged for analysis. Images were scored 1–4 (where 4 indicates better healing) based upon the extent of wound closure in the dermis and subcutis, extent of fibrosis, and the severity of inflammatory cells. At Day 7 a score of 4 = Connection of skin edges, mild inflammation and/or fibrosis; 3 = Connection of skin edges, moderate inflammation/fibrosis; 2 = Connection of skin edges, severe inflammation and/or fibrosis and presence of necrotic tissue; and 1 = non-connected skin edges. At Day 15 a score of 4 = Dermal edges connected by a scar which is ≤ 1 mm and presence of mild inflammation/fibrosis; 3 = Dermal edges connected by a scar which is ≤ 4 mm and moderate inflammation and/or fibrosis; 2 = Incomplete dermal connections, a scar ≥ 4 mm, severe inflammation and/or fibrosis, and presence of necrotic tissue; and 1 = non-connected skin edges.

In the nerve block model, the sciatic nerve was cut in the middle (transverse plane), fixed in 10% formalin and processed in paraffin. Following sectioning, 2 sequential slides were stained, the first stained with H&E and the second using immunohistochemical staining with myelin basic protein antibody for assessment of nerve myelination. The sciatic nerve sections were scored by a pathologist 0–3 where 0 = No evidence of damage; 1 = Mild damage with < 10% of neural tissue is affected; 2 = Moderate damage where 10–50% of neural tissue is affected; and 3 = Severe damage > 50% of neural tissue is affected. Note the scoring is opposite of that in the incisional model.

Statistical assessment

In *vitro* release testing, distress behavioral scoring, and time to approach utilized a two-way ANOVA followed by a Tukey's post hoc comparison of all groups at each timepoint. For Von Frey raw data and AUC values, individual datapoints were reciprocally transformed to normalize before a two-way ANOVA with a Tukey's post-hoc at each timepoint was performed. Mean peak bupivacaine concentration in plasma (C_{max}) and mean area under pharmacokinetic profile curves (AUC and AUC/D), as represented in Table 3 & 4, each utilized a one-way ANOVA with a Tukey's post-hoc. Histological scoring was analyzed with a student T-test within treatment groups between 7 and 15-day timepoints and using a one-way ANOVA with a Dunnett's multiple comparison to bupivacaine HCl at each timepoint. All analysis

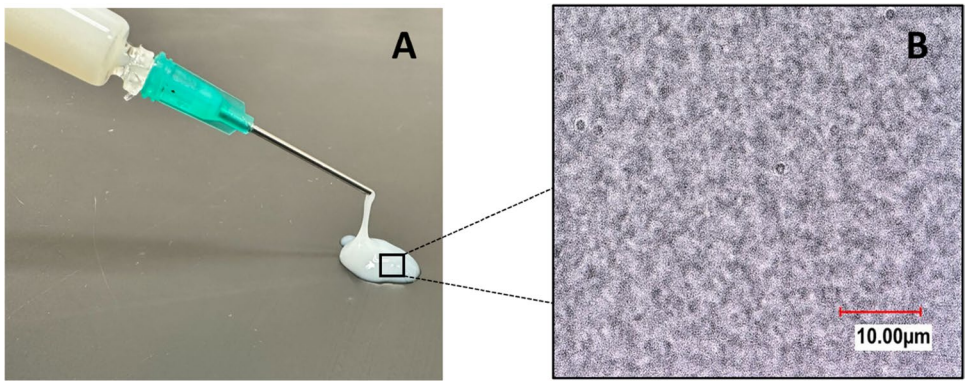

Fig. 1 Benchtop characterization of 5.4% ALX005 oleogel bupivacaine formulation. **A** Macroscopic image of 5.4% ALX005 after injection onto a benchtop. **B** Brightfield light microscopy image of 5.4% ALX005 oleogel structure with tristearin crystalline network (Scale bar 10 µm)

was performed with $\alpha = 0.05$ using Prism GraphPad version 10.0.2, and graphical representation of data is presented in standard error mean (SEM).

Results

Characterization of oleogel design in vitro

Upon formulation, the product resulted in a white, semi-opaque, gel (Fig. 1A). Liquid chromatography confirmed the oleogel made with 3% (w/v) (drug/oil) yielded a final drug loading of 2.7% ± 0.19% (w/v) (bupivacaine/oleogel) and the formulation made with 6% (w/v) (drug/oil) resulted in a final drug loading of 5.4% ± 0.39% (w/v) (bupivacaine/oleogel). It is noted that no additional peaks were observed on the chromatograms which is indicative of bupivacaine stability throughout the manufacturing process. Light microscopy images of 5.4% ALX005 at 5000x show the network of the self-assembled tristearin gelator crystals that structured the oil into a physical gel (Fig. 1B).

X-ray diffraction (XRD) profile of 5.4% ALX005 resulted in a large amorphous hump along with sharp peaks (Fig. 2A). This is indicative of the semisolid structure of an oleogel that has distinct crystalline structures within it [33, 50]. XRD confirms that tristearin is crystalizing as its signature peaks at 6°, 19°, 23°, and 25°(2θ) are the only distinctive peaks found in the ALX005 oleogel. Most of the peaks are below 25° (2θ), indicating the crystalline structures are forming with relatively large interplanar scaling. As no peak shifts are occurring from the powder form of tristearin, it provides evidence that the crystal form of the tristearin is unchanged and structuring is occurring due to a suspended precipitation of tristearin [51]. The XRD profile of crystalline bupivacaine freebase has its largest signature peak at 9.8° (2θ). This profile does not appear in the ALX005 oleogel, providing evidence that the bupivacaine is fully solubilized in the oil.

DSC method revealed the melting point of the tristearin, bupivacaine, and the oleogel formulation 5.4% ALX005 to be 78.4℃, 93.1–111.5℃, and 57.8℃, respectively (Fig. 2; B1-B3). Bupivacaine was found to have multiple peaks suggesting multiple crystalline structures. It is noted, that the manufacturing method utilizes a temperature that is 13℃ lower than the melting point of the bupivacaine but 2℃ above the melting point of tristearin. The melting temperature of ALX005 is well above 37℃, indicating thermal stability at room temperature and in vivo physiological temperatures. However, when cooled from a melted state, the oleogel has a recrystallization temperature of 27.7℃. The viscosity curves of 5.4% ALX005 oleogel have a steep downward slope as shear rates increase, indicative of shear-thinning behavior (Fig. 2C & D). As shear rates increase, measured viscosity decreases by two orders of magnitude from 26,586 ± 1,230 mPa•s and 27,140 ± 631 mPa•s at shear rate of 1 s^{-1} to 496 ± 7 mPa•s and 237 ± 4 mPa•s at a shear rate of 470 s^{-1} at 20℃ and 37℃, respectively. Temperature has a slight effect on the fluidity of the oleogel which can be seen at the low shear rates (0.1 – 0.7 s^{-1}) as the 20℃ is trending towards a zero-shear viscosity plateau, whilst the 37℃ group remains linear in this region [52].

Ideally, ALX005 would be able to be used in both local and regional administrations; therefore, its ability to be injected through a peripheral nerve block catheter and 4-inch needle was also assessed (Fig. 2E). A 15-inch catheter with a 4-inch needle were chosen to simulate the largest injection forces required because these are considered the upper end of catheter and needle length used in the clinic for peripheral nerve blocks. Without the use of a needle, injection through a 15-inch, 1 mm inner diameter, catheter resulted in forces 23.0 ± 0.4 N. Injection forces increased steadily following smaller diameter needles with 18G, 20G, and 21G needles resulting in forces of 33.4 ± 0.8 N, 49.8 ± 2.0 N, and 68.1 ± 2.2 N, respectively. Oil binding capacity is an assay used to assess the general homogeneity and stability of oleogels (Fig. 2F). Oil binding capacity was found to be 97.9% ± 1.4% after injection through a 18G needle, which is indicative of a robust oleogel that can withstand injection forces without breaking down.

In vitro drug release testing was performed to understand the effects of drug concentration and administered volume

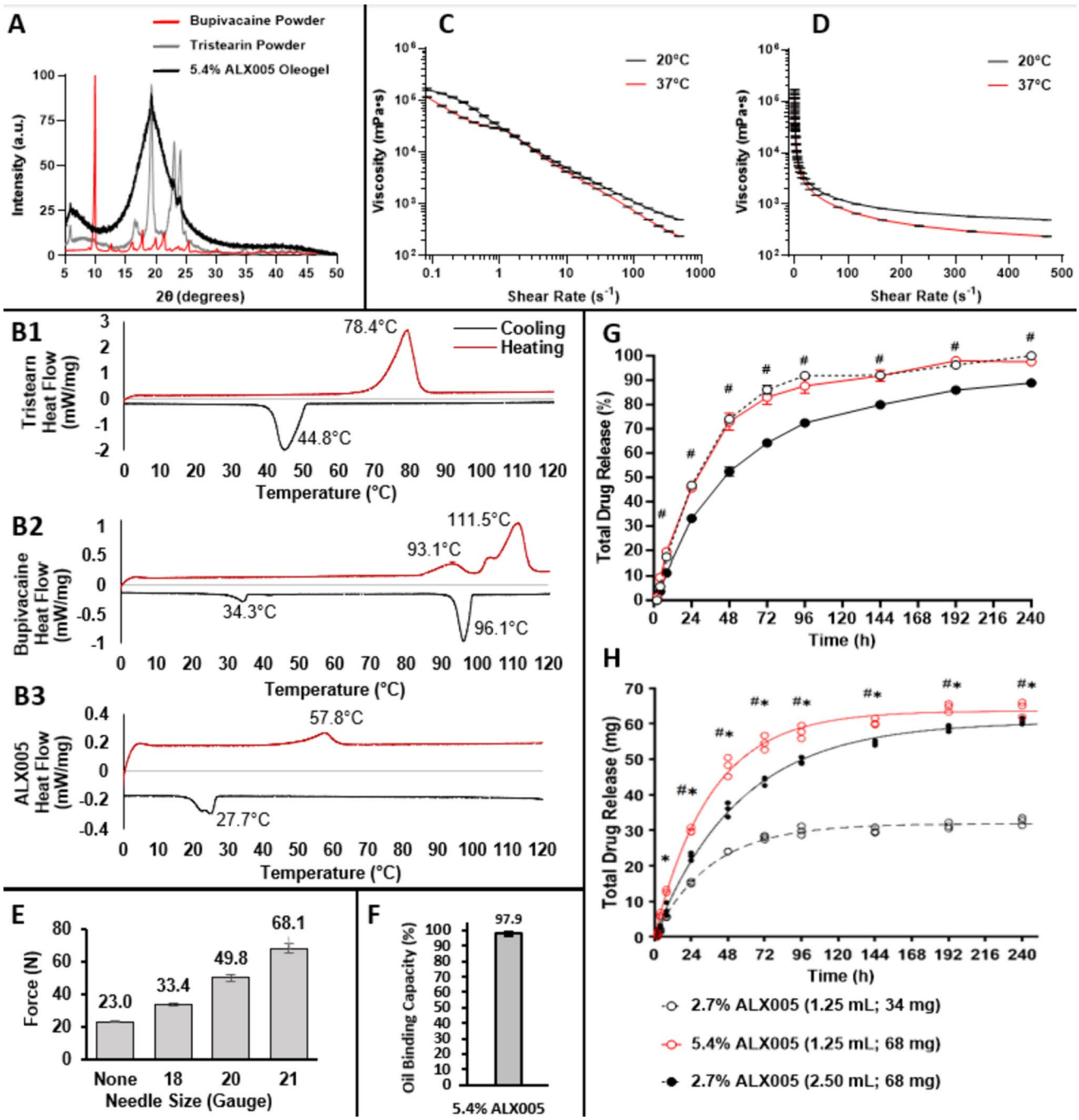

Fig. 2 **A** X-ray diffraction profiles of tristearin powder, bupivacaine freebase powder, and 5.4% ALX005 oleogel. **B1, B2, B3** Dynamic scanning calorimetry heat and cooling curves of tristearin, bupivacaine freebase and 5.4% ALX005 oleogel formulation, respectively. **C** Viscosity curves of 5.4% ALX005 with logarithmic x-axis. **D** Viscosity curves of 5.4% ALX005 with linear x-axis. **E** Force applied during injection of 5.4% ALX005 through 15-inch catheter and various gauged 4-inch needles. **F** Oil binding capacity of 5.4% ALX005 (**G**) In vitro cumulative release of 2.7% and 5.4% ALX005 oleogel formulations. **H** Mathematical model fit (lines) to raw data (circles) of in vitro release by cumulative mass released. Statistical assessment for in vitro release test denoted where * indicates statistical difference between 2.7% ALX005 1.25 mL and 5.4% ALX005 1.25 mL and # indicates statistical difference between 2.7% ALX005 1.25 mL and 2.7% ALX005 2.50 mL at denoted timepoint

on the bupivacaine release profile of ALX005 (Fig. 2G & H). To understand concentration and volume dependence the Hixson and Crowell's modified version of the Noyes-Whitney first-order mathematical equation (Eq. 2) was chosen to quantify and model total mass release characteristics (the lines in Fig. 2H). The model goodness of fit was assessed using

Table 2 Coefficients from Hixson and Crowell's first-order mathematical equation model fit for cumulative milligram released in vitro release test (top). Goodness of fit statistical metrics Standard Error of the Estimate (Sy.x), Root Mean Square Error (RMSE), and the Akaike Information Criterion (AIC) (bottom)

	2.7% ALX005 (1.25 mL)	2.7% ALX005 (2.5 mL)	5.4% ALX005 (1.25 mL)
M_{Depot} (mg)	31.8	60.4	63.5
r ($\frac{mg}{h}$)	0.027	0.018	0.027
b (mg)	2.9×10^{-8}	2.1×10^{-8}	3.4×10^{-9}
Sy.x	0.819	0.928	0.774
RMSE	11.47	19.15	19.26
AIC	52.79	63.05	63.16

several statistical metrics including the Standard Error of the Estimate (Sy.x), Root Mean Square Error (RMSE), and the Akaike Information Criterion (AIC). The model fit values (Table 2) are relatively similar between experiments where the maximum standard deviation was found to be 2 mg/timepoint. The relatively lower Sy.x value indicates a reasonably close fit, the RMSE suggests some deviation between the observed and predicted values, and the AIC value indicates the Hixon and Crowell is an acceptable model for this study but a more optimal model likely exists.

Model coefficients M_{Depot}, r, and b, as shown in Table 2, confirm the release characteristics to be both concentration and volume dependent. Where, the first order kinetic constant (r) seems to be independent of both formulation concentration and total administered drug. Constant r remains identical when the volume is fixed, but decreases by $\frac{2}{3}$ when the volume is doubled. Indeed, the cumulative percent drug released (Fig. 2G) shows that when the administered volume is fixed at 1.25 mL, the rate of release does not change despite formulation concentration doubling (p-value > 0.05 for all timepoints). A lengthening in release rate is observed for the larger volume with a lower concentration (2.5 mL; 2.7% drug) as compared to the 1.25 mL 5.4% drug concentration even though they have the same total drug loading of 68 mg. The model confirms that a burst release (b) is not relevantly present and the release is fully dependent on sustained release from the formulation (M_{Depot}). M_{Depot} was found to be dependent on the total administered drug where, independent of formulation concentration and volume administered, M_{Depot} dropped by approximately half when the total administered drug was also halved. This can be observed in the raw data (circles in Fig. 2H) where, the milligram mass of drug coming out at each timepoint differs between the 2.7% and 5.4% concentrations at 1.25 mL. For example, at the 24-h timepoint 15.2 ± 0.3 mg and 26.1 ± 0.7 mg were released, respectively. This is also as expected as there is less drug in the 2.7% formulation as compared to the 5.4%.

Post-operative pain porcine incisional model

In vivo efficacy, behavior, and pharmacokinetic metrics

After local instillation of treatment group subcutaneously into the incision created in the lower lumbar region, von Frey filaments were applied 0.5 cm from the incisional wound to measure the efficacy and duration of effect for each treatment group (Fig. 3A).

Bupivacaine HCl provided desensitization around the wound through 1, 2, and 4 h (Fig. 3B). By hour 12, Bupivacaine HCl appears to wear off completely and the animals in this group were highly responsive to the von Frey filaments with average responses of $4.1\ g \pm 0.4\ g$ from 12 to 120 h. The low dose ALX005 (1.88 mL) was significantly more effective at providing desensitization around the wound than bupivacaine HCl at hours between 4 and 120 h (p-values < 0.05). However, at 24 h and beyond, the analgesic effect of the low dose of ALX005 (1.88 mL) appears to diminish with responses to von Frey filaments of 7.94 ± 1.3 g from 24 to 120 h. The high dose of ALX005 (3.75 mL) provided the largest degree of analgesic effect and was significantly more effective at providing desensitization around the wound compared to low dose ALX005 through hours 24, 36 and 48 and compared to Bupivacaine HCl through hours 4 -120 (p-values < 0.05). At the 96 and 120 h timepoints, high dose ALX005 (3.75 mL) had a mean response of 15.2 ± 5.8 g and 10.2 ± 2.6 g, respectively. It is noted the that the mean response of high dose ALX005 (3.75 mL) at 96 h is similar to the mean response of bupivacaine HCl treatment at 4 h (15.8 ± 8.2 g). AUC analysis of the von Frey profiles found both ALX005 treatment groups to be statistically different from Bupivacaine HCl in across all time periods (Fig. 3C). The level of analgesia and the duration of analgesia were improved for the ALX005 groups compared to the Bupivacaine HCl group in a dose-dependent manner.

Distress Behavior Scoring (Methods Section: Animal Model Metrics - Von Frey measurement of mechanical hyperalgesia) was performed to assess how the analgesic effect of the various treatment groups affected the animal's behavior and stress (Fig. 3D). In the first two hours, the low dose ALX005 (1.88 mL) group had behavior scores that were significantly higher when compared to bupivacaine HCl, with bupivacaine HCl scoring a mean of 1 ± 1.1 and ALX005 low dose (1.88 mL) scoring 2.3 ± 0.5 (p-value = 0.002). However, by hour 4, there were no differences in behavior score between the low dose ALX005 group and other treatments, and by hour 12 the low dose ALX005 was trending below bupivacaine HCl and by the 24-h timepoint, low dose ALX005 had a significantly decreased distress behavioral score (0.8 ± 0.4) compared to bupivacaine HCl (2.2 ± 0.8; p-value = 0.002) which continued through 36 h. By hour 48, low dose ALX005 and bupivacaine HCl

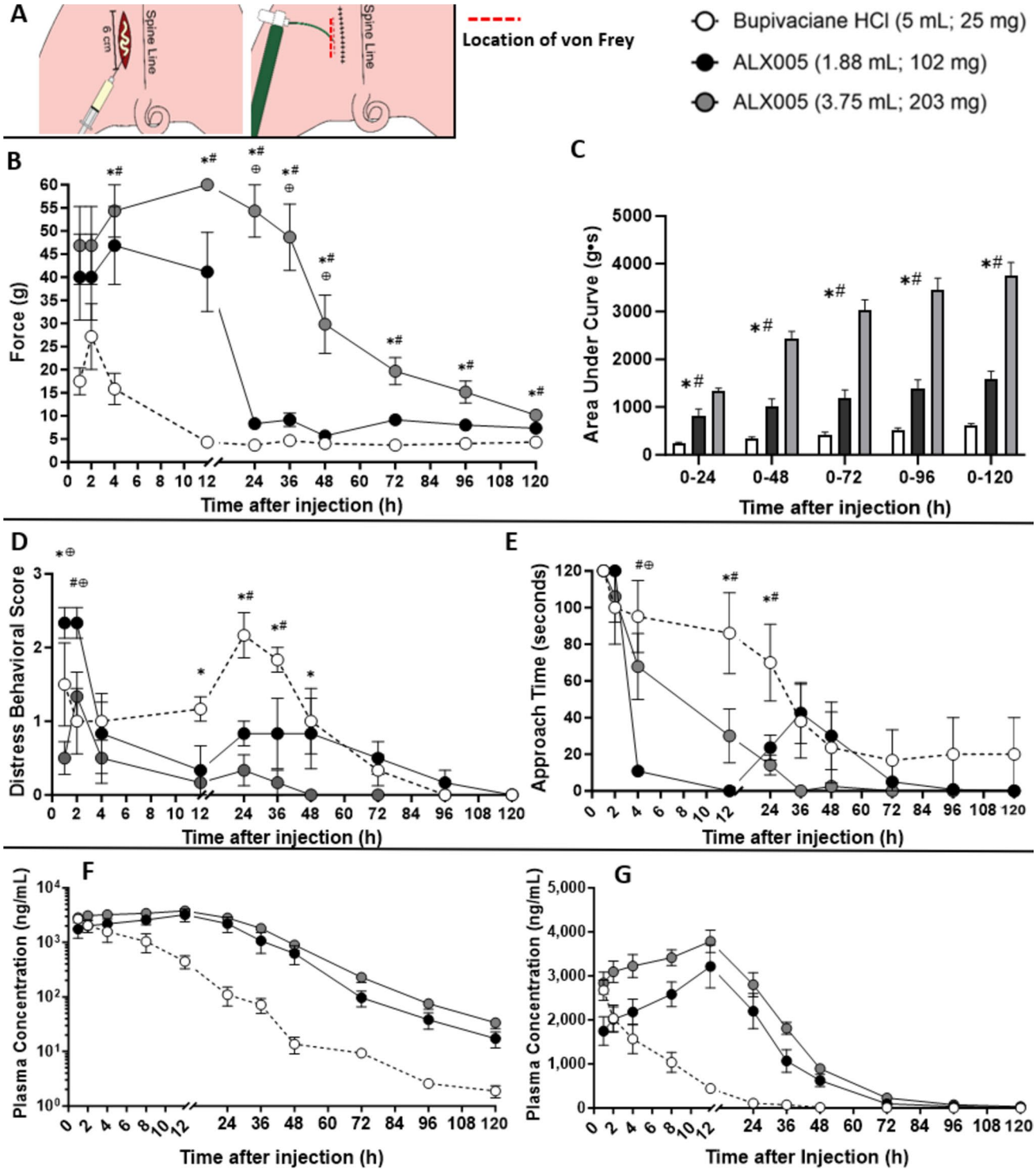

Fig. 3 In vivo metrics recorded in the incisional wound model after administration of each treatment. **A** Schematic of incisional wound model with location of drug instillation and von Frey assessment. **B** Von Frey efficacy testing 1–120 h after administration of each treatment. **C** Area under the curve (AUC) analysis of the Von Frey efficacy testing. **D** Distress behavior assessment over time. **E** The time for animal approach to researcher when entering pen. **F & G** Bupivacaine concentration in blood plasma represented in logarithmic scale and linear scale, respectively. Statistical differences denoted (**B-E** only) where * indicates that high dose ALX005 (3.75 mL) is significantly different when compared to Bupivacaine HCl (p-value < 0.05) at the denoted timepoint; # indicates low dose ALX005 (1.88 mL) significantly different when compared to Bupivacaine HCl (p-value < 0.05) at denoted timepoint; ⊕ indicates high dose ALX005 (3.75 mL) significantly different when compared low dose ALX005 (1.88 mL) (p-value < 0.05) at denoted timepoint

had similar response profiles for the remainder of the test, indicating the low dose ALX005 analgesic effect was diminishing by 48 h. High dose of ALX005 (3.75 mL) had statistical improvement of animal distress compared to Bupivacaine HCl at 1, 12, 24, 36, and 48 h (p-value < 0.05), indicating the high dose ALX005 analgesic effect lasted past 48 h. Differences between ALX005 high and low dose were most prominent in the first 2-h post-administration of treatment. The ALX005 treatments improved distress behavior scores compared to Bupivacaine HCl in a dose-dependent manner.

The time that it took each animal to approach the researcher when entering the animal's pen was recorded to further understand the effect of the various treatments on animal distress (Fig. 3E). In the first two hours there were no differences between groups. At hour 4, the low dose ALX005 (1.88 mL) had a significant decrease in approach time when compared to Bupivacaine HCl and high dose ALX005 (p-value < 0.0001 and 0.0062, respectively). Low dose ALX005 had continued significant improvement to bupivacaine HCl through 12 and 24 h timepoints (p-values < 0.0001 and 0.0329, respectively). By 36 h, an increase in approach time was observed in the low dose ALX005 as it converged and continued to follow a similar approach profile as the bupivacaine HCl group. The high dose ALX005 began trending faster approach times around 4 h (p-value = 0.2358) and by 12 h was significantly faster than bupivacaine HCl through 24 h. It should be noted the p-value for the 36-h timepoint is 0.0722 when compared to bupivacaine HCl, and through 36–120 h approach time remains nearly 0 for all animals in this group. The ALX005 treatments improved approach time compared to Bupivacaine HCl in a dose-dependent manner.

Because the pharmacokinetic arm of this study is stressful to the animals and could confound the behavioral and analgesic assays, pharmacokinetic testing was performed on the 8th day of the study after a second separate incision & administration on the contralateral side to ensure the efficacy and behavior metrics were not influenced (Methods Section: In vivo pig post-operative pain model). The bupivacaine concentration found in blood plasma at predetermined timepoints is shown in Fig. 3 (F&G) while pharmacokinetic metrics including maximum bupivacaine concentration, time to maximum bupivacaine concentration, area under the curve, and half-life can be found in Table 3.

Though no statistical differences were found in C_{max} amongst the treatment groups. The time to maximum concentration (T_{max}) for bupivacaine HCl was 1 h. Both 1.88 mL and 3.75 mL ALX005 treatments have a similar pharmacokinetic profile with peak concentration (T_{max}) occurring at 12 h post-instillation. The half-life ($t_{1/2}$) of the ALX005 groups was roughly 4-times as long as the bupivacaine HCl. AUC_{inf} comparisons between ALX005 formulations resulted in a p-value of 0.1235. The area under the curve (AUC_{inf}) for low and high ALX005 treatments were both higher than that of bupivacaine HCl (p-value = 0.0069 and 0.0009, respectively). In contrast, when the AUC_{inf} were normalized to administered dose of bupivacaine per kilogram of animal (AUC_{inf}/D), both ALX005 groups were found to have no statistical differences to bupivacaine HCl (p-values = 0.9897 & 0.2586 for low and high ALX005, respectively) (Table 3).

Histological assessment

Upon sacrifice, the incision and treatment administration sites were harvested and the histological sections were scored (Methods Section: Animal Model Metrics - Histological assessment) at 7-days and 15-days post-administration of each treatment. Representative photos from each group can be found in Table 3. Histological score results are shown in Fig. 4.

By day 15, the incisional wounds of all groups were fully re-epithelialized. Fibrinopurulent debris can be seen on the outer edges of the incision. Subcutaneously, fibrotic dermal tissue is present representative of healing recently injured dermal tissue. Lipid granulomas surrounded by inflammatory cells were observed sub-dermally in the ALX005 groups, which can be the remaining presence of the lipid oleogel formulation. Histological scores indicate that at the 7-day timepoint there were no differences in the rate at which the wounds were healing regardless of treatment.

Table 3 Mean peak concentration of bupivacaine in the plasma (C_{max}), time to peak bupivacaine concentration in the plasma (T_{max}), the mean area under the curve (AUC) of the entire pharmacokinetic profile, the mean area under the curve of the pharmacokinetic profile normalized to milligram dose of bupivacaine received (AUC/D), and half-life. All in Mean ± STD. Statistical differences denoted where * indicates that a significant difference exists when compared to Bupivacaine HCl (p-value < 0.05)

Treatment Group	$C_{max}\left(\frac{ng}{mL}\right)$	T_{max} (h)	$AUC_{inf}\left(h * \left(\frac{ng}{mL}\right)\right)$	$\left(h * \frac{\left(\frac{ng}{mL}\right)}{\frac{mg}{kg}}\right)$	$t_{1/2}$ (h)
Bupivacaine HCl (5 mL; 25 mg)	2,677 ± 402	1 ± 0	20,943 ± 6,172	11,875 ± 2,848	5.14 ± 0.35
ALX005 (1.88 mL; 102 mg)	3,217 ± 847	12 ± 0	101,815 ± 29,751*	11,638 ± 1,819	20.9 ± 2.7*
ALX005 (3.75 mL; 203 mg)	3,783 ± 441	12 ± 0	141,289 ± 18,264*	8,834 ± 1,391	21.7 ± 1.4*

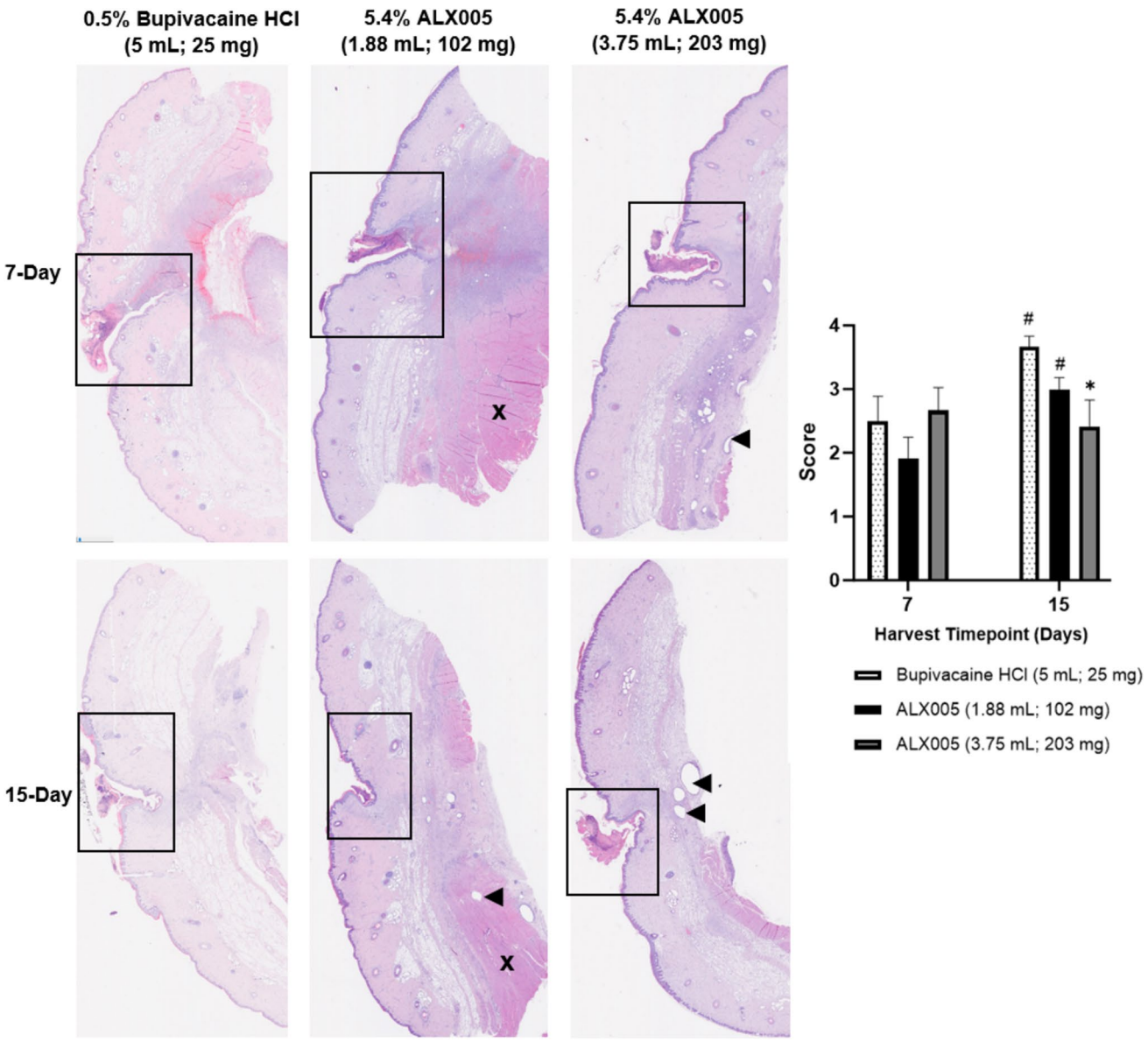

Fig. 4 Representative images of histological sections of incisional wound following administration of bupivacaine HCl or ALX005 (left). Black box indicates area of wound closure; ▲ indicates lipid droplets; **x** indicates section of muscle. Histological score (right) within treatment groups between 7 and 15-day timepoints (right). Statistical differences denoted where * indicates a significant difference from bupivacaine HCl at the same timepoint and # indicates a significant difference within the same treatment group at 7-day compared to 15-day

At 15-days, bupivacaine HCl had healed significantly faster than ALX005 high dose (3.75 mL) (p-value = 0.0121) but no differences were found between bupivacaine HCl and the low dose ALX005 (1.88 mL). Both bupivacaine HCl and ALX005 low dose (1.88 mL) had a significant improvement in wound healing after 15-days when compared to 7-days (p-values = 0.0199 and 0.0160, respectively). ALX005 high dose (3.75 mL) did not have significant changes in wound healing between 7 and 15 days.

Sciatic nerve block model

Efficacy, behavior and pharmacokinetic metrics

An ultrasound was used to guide the placement of the nerve block (Fig. 5A). After guided injection of treatment groups perineurally to the sciatic, von Frey filaments were applied approximately 0.5 cm from the incisional wound created on the distal lateral of the hind leg to measure the

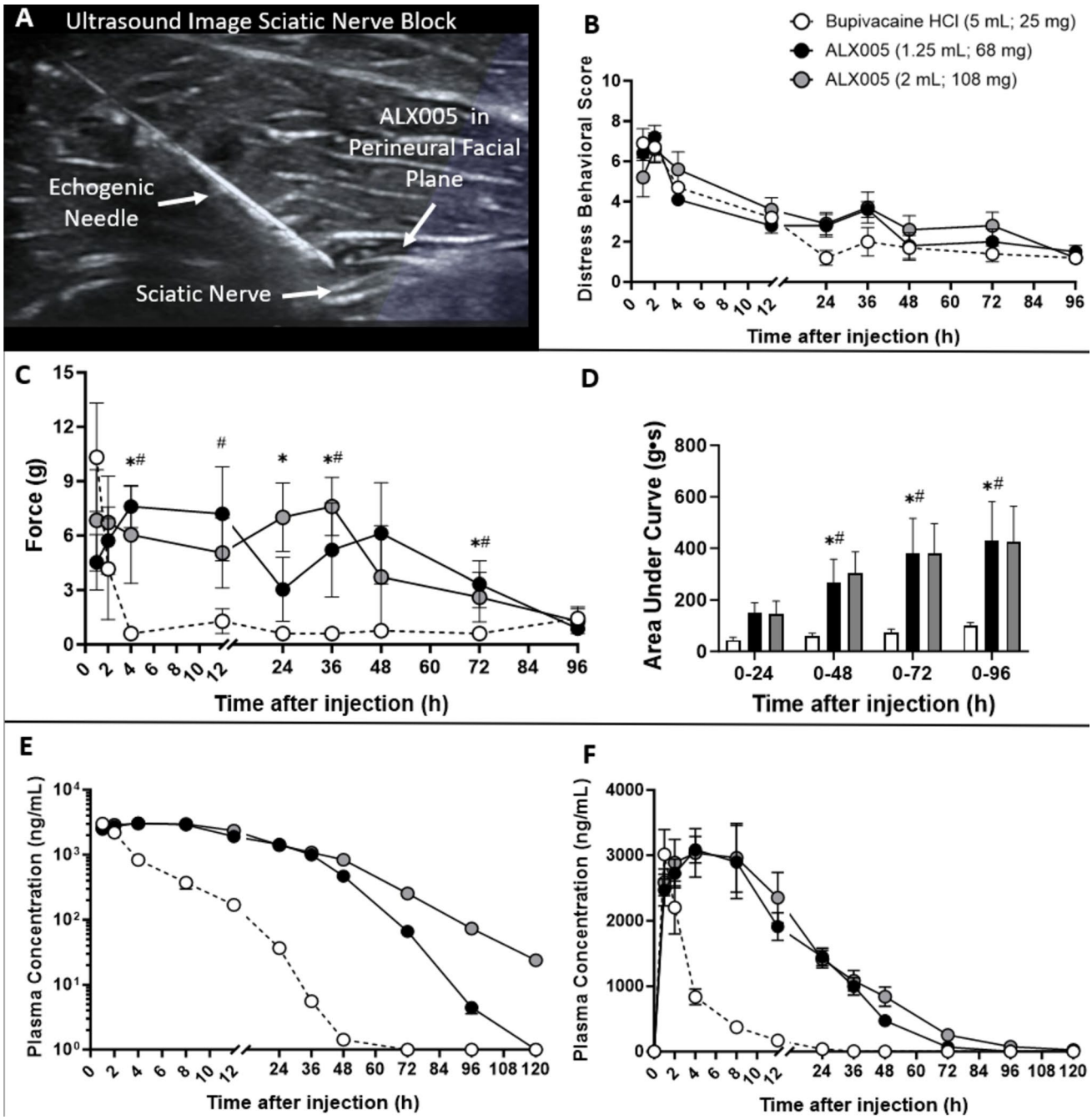

Fig. 5 In vivo metrics recorded in the sciatic nerve block model after administration of each treatment. **A** Ultrasound image of injection site for treatment groups. **B** Distress behavior assessment over time. **C** Von Frey efficacy over time. **D** Von Frey AUC through different timespans. **E&F** Bupivacaine concentration in blood plasma represented in logarithmic scale and linear scale, respectively. Statistical differences denoted (**B-D** only) where * indicates that high dose ALX005 (3.75 mL) is significantly different when compared to Bupivacaine HCl (p-value < 0.05) at the denoted timepoint; # indicates low dose ALX005 (1.88 mL) significantly different when compared to Bupivacaine HCl (p-value < 0.05) at denoted timepoint; ⊕ indicates low dose ALX005 (1.88 mL) significantly different when compared high dose ALX005 (3.75 mL) (p-value < 0.05) at denoted timepoint

efficacy and duration of effect of the nerve block for each treatment group.

The general distress of animals, after ultrasound guided nerve block injection of treatment groups perineurally to the sciatic, was evaluated using behavioral monitoring and the Distress Behavior Scoring (see Methods Section: Animal model metrics - Distress behavior scoring) (Fig. 5B). No differences were found in the animal's behavior between any of

the treatment nerve block injection group over the course of this experiment. Efficacy of treatment groups was assessed utilizing the von Frey test (Fig. 5C). Bupivacaine HCl provided desensitization around the wound for the first 2 h after administration but wore off by the 4 h timepoint after which the animals in this group were highly responsive to the von Frey filaments with average responses of 0.84 g ± 0.4 g over 4 to 96 h. No differences were found between groups in the first 2 h of assessment. At hour 4, both high and low dose ALX005 (1.25 mL and 2 mL, respectively) had significantly higher von Frey responses than bupivacaine HCl through the 72-h timepoint. No statistical differences were found between the low and high dose ALX005 in either the von Frey raw data or AUC data (Fig. 5D). However, both low and high dose ALX005 were found to have statistically larger AUC than bupivacaine HCl through timespans after 48 h.

In the same fashion as the incisional model, the pharmacokinetic arm of the nerve block model was performed on the 8th day of the study after a second, separate, surgery to ensure the efficacy and behavior metrics were not influenced (Results Section: Post-operative pain porcine incisional model). The bupivacaine concentration found in blood plasma at pre-determined timepoints is shown above (Fig. 5E & F). Administration of 1.25 or 2 mL of ALX005 resulted in similar plasma bupivacaine pharmacokinetic profiles. The two doses appeared to release at the same rate, with the higher volume having a longer release time. Notably, administration of ALX005 gave bupivacaine doses 2.7 and 4.3-fold higher than bupivacaine HCl but did not result in significantly different plasma C_{max} values (Table 4).

Both ALX005 treatments had a T_{max} of 6.7 h. The half-life of ALX005 was found to be significantly greater than bupivacaine HCl; however, it was found that the half-life of ALX005 increased in a dose-dependent manner. The area under the pharmacokinetic curves (AUC) were found to be significantly larger than that of bupivacaine HCl. In contrast to results from the incisional model, when the AUC were normalized to administered dose of bupivacaine per kilogram of animal, both ALX005 groups were found to have statistical differences to bupivacaine HCl (Table 4).

Histological assessment

Upon sacrifice, sciatic nerves were harvested at injection site and the histological sections were scored (Method Section: Animal model metrics - Histological assessment) at 7-days and 15-days post-administration of each treatment. Representative photos and score results are described in Fig. 6.

At the 7-day timepoint, all three study groups had one animal per group with mild findings in the sciatic nerve where a small groups of nerve bundles appeared necrotic. At the 15-day timepoint, mild gliosis was found in a single animal treated with high dose of ALX005. All other tissues were scored 0, indicative of no evidence of damage found. Upon histological scoring, no statistical differences were found between groups at either 7-day or 15-day. Furthermore, no differences were found within treatment groups between 7 and 15-day.

Discussion

Opioids-based medications for post-operative pain management are associated with the development of opioid use-disorders, accidental overdose, and adverse events that can prolong hospitalization and increase cost of care [1, 2, 4, 6]. Local anesthetic drugs such as bupivacaine and ropivacaine are effective at controlling the intense pain after surgery, but their duration is limited to roughly 6–24 h, depending on the application and dose [14]. Increasing the duration of local anesthetic via controlled-release drug delivery technology has been a hot topic of research and commercial development activities over the last few decades [16]. The goal of this research is to create a drug product that can provide multiple days of extended local anesthetic release to control post-operative pain locally with a single administration and bridge patients across the initial 72-h period of intense pain where opioids are most needed. Other critical factors that affect a long-acting local anesthetic's ultimate clinical utility are cost, versatility of use, and ease of use. The ideal long-acting local anesthetic drug product should provide

Table 4 Mean peak concentration of bupivacaine in the plasma (C_{max}), time to peak bupivacaine concentration in the plasma (T_{max}), half-life ($t_{1/2}$) the mean area under the curve (AUC) of the entire pharmacokinetic profile, and the mean area under the curve of the pharmacokinetic profile normalized to milligram dose of bupivacaine received (AUC/D). All mean ± STD. Statistical differences denoted where * indicates that significantly differences exist when compared to Bupivacaine HCl (p-value < 0.05)

Treatment Group	$C_{max}\left(\frac{ng}{mL}\right)$	T_{max} (h)	$AUC_{inf}\,(h * (\frac{ng}{mL}))$	$(h * \frac{\left(\frac{ng}{mL}\right)}{\frac{mg}{kg}})$	$t_{1/2}$ (h)
Bupivacaine HCl (5 mL; 25 mg)	3,017 ± 660	1 ± 0	12,199 ± 2,958	5,997 ± 1,347	5.2 ± 0.4
ALX005 (1.25 mL; 68 mg)	3,440 ± 300	6.7 ± 2.3*	82,166 ± 11,901*	14,440 ± 2,356*	7.2 ± 0.6*
ALX005 (2 mL; 108 mg)	3,177 ± 715	6.7 ± 2.3*	100,337 ± 15,311*	10,516 ± 1,485*	12.4 ± 0.7*

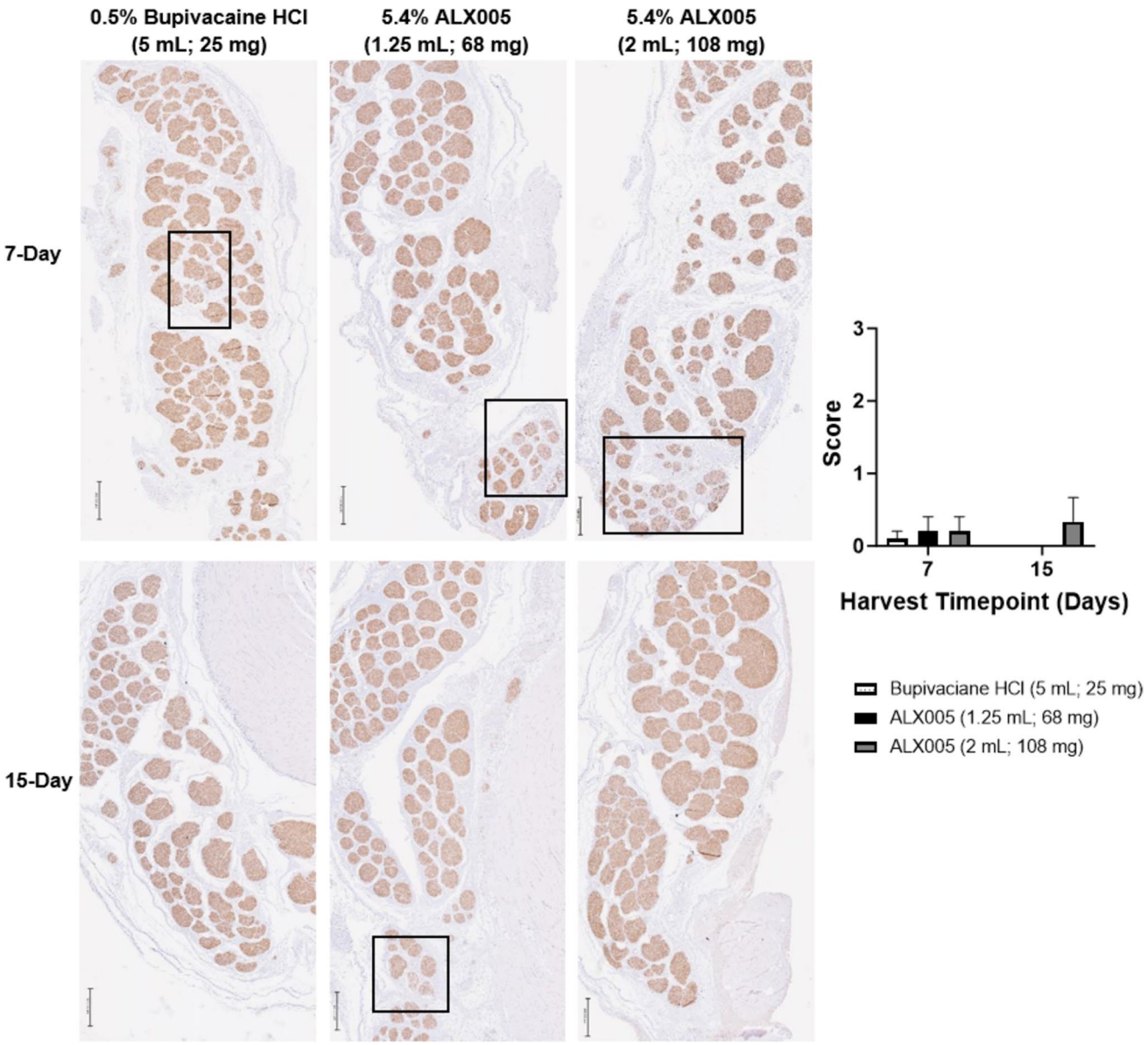

Fig. 6 Representative myelin basic protein-stained images of histological sections of sciatic nerve following perineural injection of Bupivacaine HCl or ALX005 oleogel. Black box indicates areas of necrotic tissue. Scale bar 100 μm. Histological score (right) within treatment groups between 7 and 15-day timepoints. Statistical differences denoted where * indicates a significant difference from Bupivacaine HCl at the same timepoint and # indicates a significant difference within the same treatment group at 7-day compared to 15-day

multiple days of analgesia (i.e., 72–96 h), have a rapid onset, be ready-to-use, utilize current administration techniques, low costs, and be able to be used both locally at a surgical site via instillation administration or injected percutaneously in regional anesthesia applications, such as peripheral nerve blocks. The current clinically available long-acting local anesthetics do not meet all these requirements and have technological design limitations that have prevented their widespread clinical adoption.

Liposomal bupivacaine (Exparel®) is the current best-selling long-acting local anesthetic product, however, it is only used in a small portion of surgical procedures. This is primarily driven by its debated efficacy and high costs, which has led customers to question its clinical value [17, 18, 53]. The questionable efficacy and high-cost insufficiencies can be attributed to the drug delivery technology, multivesicular liposomes [32]. The drug release from these liposomes is primarily erosion-based, which leads to delayed onset and variable release rates depending on the in vivo milieu of the administration site [42]. Additionally, manufacturing bupivacaine-loaded multivesicular liposomes is a complicated process that has to be done in aseptic

conditions because they cannot be terminally sterilized. These technological-based issues lead to a drug product with debated efficacy and high cost, which has made the customer question the true clinical value and prevented widespread adoption [17, 18, 53]. The other commercially available long-acting local anesthetic products include an extended-release bupivacaine polymeric gel (Zynrelef®), an extended-release bupivacaine sucrose acetate isobutyrate gel (Posimir®), and an extended-release bupivacaine collagen implant (Xaracoll®). All of these products have yet to gain significant clinical adoption with sales significantly lower than Exparel®. Zynrelef® has demonstrated arguably the best clinical analgesic effect and duration; however, time consuming preparation steps, the inability to be applied as a peripheral nerve block, and high costs have limited its adoption [21]. Posimir® has only shown marginal improvement in pain scores versus placebo groups and has yet to show significant improvement in clinical trials versus bupivacaine HCl controls [54]. Additionally, risk of local and systemic toxicity issues with Posimir® have led to significant warnings on their label and limited their indications for use. Zynrelef® and Posimir® are both in situ gelling depots that contain significant amounts of organic solvents, which can cause local toxicity and prohibit their use adjacent to peripheral nerves [55, 56]. Xaracoll® has only demonstrated 24 h of superior analgesic effect when compared to placebo in clinical trials [22]. Since it is a solid implant, it can only be applied into open surgical wounds, which limits its potential surgical applications. Although progress has been made with the FDA approval of multiple long-acting local anesthetic products, there is still more to be desired and an unmet clinical need for a versatile, safe, effective, and affordable long-acting local anesthetic for post-operative pain.

In order to address this unmet clinical need, we developed a novel oleogel-based injectable extended-release bupivacaine system (ALX005) made solely of low-cost GRAS, IID-listed lipid ingredients that can provide multiple days of first-order diffusion-based bupivacaine release, be applied locally or injected as a regional anesthetic, has a simple scalable manufacturing process, can be terminally sterilized and stored at room temperature. High drug loading, and therefore dose, are critical for single-administration long-acting local anesthetic products in order to maintain a therapeutic concentration over a multi-day period. Light microscopy found no presence of bupivacaine crystals (Fig. 1B) and complete elimination of bupivacaine peaks were observed on XRD analysis (Fig. 2A), indicating that complete solubility was achieved with the 5.4% bupivacaine ALX005 formulations. The XRD data also confirms the presence of a network of crystalline tristearin gelator structures (Fig. 2A). These results are in line with the work of Larsen et. al, where the solubility limit of bupivacaine in these oils was found to be above the manufactured concentration of 5.4% (w/w) and there was no preliminary evidence of bupivacaine degradation [57–59].Oil binding capacity demonstrates the formation of a robust oleogel (Fig. 2F) [40, 60]. DSC analysis found a melting point of 57.8℃ which implies that the ALX005 formulation retains its oleogel structure and is thermostable at room and in vivo temperatures (Fig. 2; B3).

ALX005 was designed to have a semi-solid structure with soft pliable characteristics that could be injected yet still be robust enough to remain at the site of administration. It has been shown that viscosity and phase play a role in extended-release and retainment of the dose at the administration site [33, 38, 61–63]. However, implants that are too rigid have been shown to augment local toxicity due to deleterious mechanical forces on fragile biological tissue [62, 64]. Therefore, the goal was to create an injectable gel that was viscous enough to retain at the site of administration to provide local extended-release of bupivacaine but not so viscous that it would induce unnecessary local toxicity. Rheological assessment found ALX005 to be highly shear-thinning (Fig. 2C & D), which enables injectability via the reduction of viscosity when shear forces are applied and then viscosity rebounds to its native state to create a local depot after injection. It was observed that injection forces increased with the use of smaller diameter needles. Limitations of injectability were found using a 4-inch 21G needle with the 15inch by 1 mm inner diameter catheter when injection forces reached and average of 68.9 N. It has been found that forces above 65 N are considered “uninjectable” [39]. In vitro drug release testing found ALX005 to have a first-order diffusion-based drug release profile with roughly 90% of the drug releasing within the first 120 h (Fig. 2G & H). The Hixson and Crowell’s model (Eq. 2) verified that burst release is not occurring and the drug release is follows a first-order diffusion-based release profile [44, 65]. Where, initial drug release rates are higher, and then slowly taper overtime as the drug concentration inside the gel reduces. A first-order diffusion-based drug release profile is ideal for long-acting local anesthetic technologies because robust early onset is desired to initiate early analgesia followed by a tapering effect over 4–5 days as post-operative pain reduces, returning sensation and motor function to the region. This is a significant advantage of erosion-based drug delivery systems, such as liposomal bupivacaine which has a delayed onset [66]. Inadequate management of intense acute pain can lead to allodynia, the perception of inadequate pain management even after effective anesthesia is achieved, and chronic pain [67].

The optimized 5.4% bupivacaine ALX005 formulation was evaluated in two separate translational pig post-operative models to assess its safety and efficacy in two different clinically-relevant routes of administration: local

instillation and peripheral nerve block. In the incisional model, ALX005 had a sustained, dose-dependent analgesic effect as demonstrated by the von Frey assay, where the high dose of ALX005 had an analgesic effect lasting approximately 120 h and the low dose ALX005 lasting approximately 24 h (Fig. 3B). The analgesic effect as demonstrated by von Frey for the bupivacaine HCl control group wore off by 12 h (Fig. 3B). Both ALX005 groups had improved distress behavior scoring and approach times compared to the bupivacaine HCl control group in a dose-dependent manner, indicating that the ideal therapeutic dose for this model is closer to the higher dose ALX005 (Fig. 3D & F). In the sciatic nerve block model, both the high and low ALX005 doses were effective through 72 h as demonstrated by the von Frey assay, but the high dose resulted in a more continuous and sustained effect (Fig. 5C). Distress behavior scores in the sciatic nerve block model were statistically similar across all groups, which can be attributed to the fact that the animals had increased stress caused by the motor and sensory paralysis of their hind leg. We found ALX005 to provide up to 2.8 and 3.5 days longer duration of anesthetic effect than bupivacaine HCl in the sciatic nerve block and incisional wound models, respectively.

Pharmacokinetic assessment was performed to characterize the in vivo extended-release profile and to understand the systemic toxicity of the bupivacaine and safety profile of ALX005 (Fig. 3F & G; Fig. 5E & F). Local anesthetic systemic toxicity is a primary safety concern when using local anesthetic drugs in the clinic. Since long-acting local anesthetic products will have increased drug payload to maintain a therapeutic concentration over an extended period of time, if the drug is released too quickly it can potentially cause local anesthetic systemic toxicity. Notably, in the incisional model, the low dose ALX005 doses fourfold higher than bupivacaine HCl but resulted in similar C_{max} values and the high dose ALX005, dosed eightfold higher, resulted in a larger C_{max} but only 1.4-fold compared to bupivacaine HCl. In the nerve block model, no differences between C_{max} values were found. Instead, low and high dose ALX005 have similar profiles with the high dose exhibiting a longer extended-release profile. The T_{max} in both models was significantly later than bupivacaine HCl, which can be attributed to the controlled-release nature of the oleogel drug delivery system. The pharmacokinetic profiles of ALX005 high and low dose were relatively similar in both pig models even though there was a large difference in administered dose. It's likely that local and systemic pharmacokinetic absorptions, volumes, and clearances affected the release, local and systemic clearance of the drug. The ALX005 formulation utilizes all GRAS lipids, primarily natural vegetable-derived triglycerides that are found in common dietary fats which are readily metabolized and degraded [68]. For single-administration long-acting local anesthetic products, biocompatibility and quick biodegradation times are desired to not cause unnecessary local toxicity at the administration site. Histological scores in both models indicate that at the 7-day timepoint all of treatment groups have similar wound healing and local toxicity profiles (Figs. 4 & 6). This trend continues through 15-day in the nerve block model, but in the incisional model high dose ALX005 (3.75 mL) was the only treatment to not have a change in wound healing from day 7 to day 15. This may be caused by excessive mechanical pressures exerted on the tissue by the high administered volume under a fresh incisional wound and extended foreign body reaction duration associated with the longer biodegradation profile of the higher volume [69]. By day 15 in both models, the low dose ALX005 formulation was completely biodegraded and only small remnants remained in the high dose ALX005 group, particularly in the incisional wound model. This degradation profile allows enough time for the formulation to remain relatively intact across the first 3–5 day window when the drug payload is delivered, but degrades rapidly enough to prevent chronic foreign body reaction [69].

This study demonstrated that an oleogel-based long-acting local anesthetic preparation has the potential to create a safe, effective, and economical solution for post-operative pain. However, this technology is still in the proof-of-concept stage and further nonclinical toxicology, including a fully validated bioanalytical protocol for the assessment of plasma storage conditions in the animal model being used, an extensive histological study, and clinical studies will need to be performed to better understand its safety, efficacy, and ultimate clinical potential for providing multi-day non-opioid analgesia. Preliminary stability has been assessed in some of our previous work [33], however a more robust and controlled stability study will need to be executed to better understand crystallization characteristics, including of precipitation events or the presence of amorphous structures as well as any changes in viscosity or release profile. A robust stability study around the active pharmaceutical ingredient bupivacaine will need to be performed to ensure bupivacaine is not precipitating out over time or degrading in ALX005 over time. Additionally, manufacturing and stability optimization will need to be performed to demonstrate that ALX005 will meet the quality requirements for regulatory approval.

Conclusion

In this manuscript we demonstrated that an oleogel-based long-acting local anesthetic preparation has potential of producing a safe, effective, and economical solution for post-operative pain. We identified an oleogel formulation (ALX005) that has an extended in vitro and in vivo drug

release with shear-thinning mechanical properties that allows injection through standard catheter-based applications, as well as being viscous enough to easily coat a wound cavity and provide direct effect through local instillation. Using standardized pig post-operative pain models, we found that ALX005 provided 2.8 and 3.5 days longer duration of anesthetic effect than bupivacaine HCl in the porcine nerve block and incisional models, respectively. Despite ALX005 bupivacaine dose 8.1 times higher than the bupivacaine HCl control dose, pharmacokinetic assessment showed that the C_{max} of high dose ALX005 treatment was only 1.4 times higher than the bupivacaine HCl control. Only minor histological changes were observed in both models compared to the bupivacaine HCl control. This study demonstrates that an oleogel-based technology has potential to be an effective injectable long-acting local anesthetic that meets the design requirements for mitigating the use of opioids after surgery.

All institutional and national guidelines for the care and use of laboratory animals were followed.

Acknowledgements X-ray diffraction, dynamic scanning calorimetry, and mechanical testing utilized the University of Utah's Materials Characterization Lab. Microscope image obtained using the University of Utah Nano Fab.

Authors contributions *Susan Wojtalewicz* Conceptualization, Study Design, Manuscript Drafting, Writing, Editing, Formatting, Data Curation, Analysis; *Jack Shuckra* Data Curation, Analysis, Manuscript Editing; *Keelah Barger* Editing, Data Curation, Analysis; *Sierra Erickson* Study Design, Editing, Formatting, Data Analysis, Conceptualization; *Jonathon Vizmeg* Data Curation, Analysis, Editing*; Stefan Niederauer* Conceptualization, Editing; *Andrew Simpson* Conceptualization, Writing, Editing; *Jordan Davis* Data Curation, Editing; *Avital Schauder* Data Curation, Data Analysis, Editing; *Orna Hifi* Study Design, Data Curation, Data Analysis, Editing; *David Castel* Study Design, Data Curation*; Sigal Meilin* Conceptualization, Study Design, Data Curation, Data Analysis, Editing; *Jayant Agarwal* Funding Acquisition, Conceptualization; *Caleb Lade* Conceptualization, Study Design, Funding Acquisition; *Brett Davis* Study Design, Manuscript Drafting, Writing, Editing, Funding Acquisition, Conceptualization.

Funding This work was supported by the National Science Foundation grants: award numbers 2233656 and 2026176.

Data availability All data will be made available upon request.

Declarations

Competing interest The authors declare the following financial interests/personal relationships which may be considered as potential competing interests: Susan Wojtalewicz, Jack Shuckra, Keelah Barger, Jonathon Vizmeg, Stefan Niederauer, Jordan Davis, Jayant Agarwal, Andrew Simpson, Sierra Erickson, Caleb Lade, and Brett Davis report financial support was provided by Rebel Medicine Inc and report a relationship with Rebel Medicine Inc that includes: board membership, employment, and/or equity or stocks. Avital Schauder, Orna Hifi, David Castel, Sigal Meilin are all employed and/or equity or stocks at MD Biosciences, a contract research organization hired by Rebel Medicine Inc to execute the in vivo work in this study.

References

1. Kessler ER, Shah M, Gruschkus SK, Raju A. Cost and quality implications of opioid-based postsurgical pain control using administrative claims data from a large health system: opioid-related adverse events and their impact on clinical and economic outcomes. Pharmacotherapy. 2013;33(4):383–91. https://doi.org/10.1002/phar.1223.
2. Brummett CM, Goesling J, Moser S, Lin P, Englesbe MJ, Bohnert ASB, Kheterpal S, Nallamothu BK. New persistent opioid use after minor and major surgical procedures in US adults. JAMA Surg. 2017;152(6):e170504.
3. Darnall BD. Incidence of and risk factors for chronic opioid use among opioid-naive patients in the postoperative period (vol 176, pg 1286, 2016), (in English). Jama Intern Med. 2016;176(9):1412–1412. https://doi.org/10.1001/jamainternmed.2016.5221.
4. Kane-Gill SL, Rubin EC, Smithburger PL, Buckley MS, Dasta JF. The cost of opioid-related adverse drug events. J Pain Palliat Care Pharmacother. 2014;28(3):282–93. https://doi.org/10.3109/15360288.2014.938889.
5. Rudd RA, Aleshire N, Zibbell JE, Gladden RM. Increases in drug and opioid overdose Deaths-United States, 2000–2014. MMWR Morb Mortal Wkly Rep. 2016;64(50–51):1378–82. https://doi.org/10.15585/mmwr.mm6450a3.
6. Oderda GM, et al. Opioid-related adverse drug events in surgical hospitalizations: Impact on costs and length of stay, (in English). Ann Pharmacother. 2007;41(3):400–7. https://doi.org/10.1345/aph.1H386.
7. Oderda GM, Gan TJ, Johnson BH, Robinson SB. Effect of opioid-related adverse events on outcomes in selected surgical patients. J Pain Palliat Care Pharmacother. 2013;27(1):62–70. https://doi.org/10.3109/15360288.2012.751956.
8. Shafi S, et al. Association of opioid-related adverse drug events with clinical and cost outcomes among surgical patients in a large integrated health care delivery system. JAMA Surg. 2018;153(8):757–63. https://doi.org/10.1001/jamasurg.2018.1039.
9. Florence CS, Zhou C, Luo F, Xu L. The economic burden of prescription opioid overdose, abuse, and dependence in the United States, 2013. Med Care. 2016;54(10):901–6. https://doi.org/10.1097/MLR.0000000000000625.
10. Barker JC, Joshi GP, Janis JE. Basics and best practices of multimodal pain management for the plastic surgeon, (in eng). Plast Reconstr Surg Glob Open. 2020;8(5):e2833. https://doi.org/10.1097/gox.0000000000002833.
11. Kaye AD, et al. Multimodal analgesia as an essential part of enhanced recovery protocols in the ambulatory settings, (in eng). J Anaesthesiol Clin Pharmacol. 2019;35(Suppl 1):S40-s45. https://doi.org/10.4103/joacp.JOACP_51_18.
12. Hartman TJ, Nie JW, Singh K. Multimodal Analgesia. Contemp Spine Surg. 2022;23(8). Available: https://journals.lww.com/cssnewsletter/fulltext/2022/08000/multimodal_analgesia.1.aspx. Accessed July 2024.
13. Zaslansky R, et al. Improving perioperative pain management: a preintervention and postintervention study in 7 developing countries, (in eng). Pain Rep. 2019;4(1):e705. https://doi.org/10.1097/pr9.0000000000000705.
14. Albrecht E, Chin KJ. Advances in regional anaesthesia and acute pain management: a narrative review. Anaesthesia. 2020;75(Suppl 1):e101-10. https://doi.org/10.1111/anae.14868.
15. Malik O, Kaye AD, Kaye A, Belani K, Urman RD. Emerging roles of liposomal bupivacaine in anesthesia practice, (in eng). J Anaesthesiol Clin Pharmacol. 2017;33(2):151–6. https://doi.org/10.4103/joacp.JOACP_375_15.

16. Kaye AD, et al. Novel local anesthetics in clinical practice: Pharmacologic considerations and potential roles for the future, (in eng). Anesth Pain Med. 2022;12(1):e123112. https://doi.org/10.5812/aapm.123112.
17. McCann ME. Liposomal bupivacaine: effective, cost-effective, or (Just) costly? Anesthesiology. 2021;134:139–43. https://doi.org/10.1097/ALN.0000000000003658.
18. Hussain N, Brull R, Sheehy B, Essandoh MK, Stahl DL, Weaver TE, Abdallah FW. Perineural liposomal bupivacaine is not superior to nonliposomal bupivacaine for peripheral nerve block analgesia. Anesthesiology. 2021;134(2):147–64. https://doi.org/10.1097/ALN.0000000000003651.
19. Vyas KS, et al. Systematic review of liposomal bupivacaine (Exparel) for postoperative analgesia. Plast Reconstr Surg. 2016;138(4):748e–56e. https://doi.org/10.1097/PRS.0000000000002547.
20. Skolnik A, Gan TJ. New formulations of bupivacaine for the treatment of postoperative pain: liposomal bupivacaine and SABER-Bupivacaine. Expert Opin Pharmacother. 2014;15(11):1535–42. https://doi.org/10.1517/14656566.2014.930436.
21. Kang RS, Jin Z, Gan TJ. A novel long-acting local anesthetic - HTX-011 (ZYNRELEF()) for postoperative pain control. Expert Rev Clin Pharmacol. 2022;15(10):1147–53. https://doi.org/10.1080/17512433.2022.2132227.
22. Hemsen L, Cusack SL, Minkowitz HS, Kuss ME. A feasibility study to investigate the use of a bupivacaine-collagen implant (XaraColl) for postoperative analgesia following laparoscopic surgery. J Pain Res. 2013;6:79–85. https://doi.org/10.2147/JPR.S40158.
23. Zynrelef. Highlights of prescribing information, HERON. 2021. https://www.accessdata.fda.gov/drugsatfda_docs/label/2021/211988s000lbl.pdf. Accessed July 2024.
24. POSIMIR. Highlights of prescribing information. Innocoll; 2021. https://www.accessdata.fda.gov/drugsatfda_docs/label/2021/204803s000lbl.pdf. Accessed July 2024.
25. Joshi GP, Janis JE, Haas EM, Ramshaw BJ, Nihira MA, Dunkin BJ. Surgical site infiltration for abdominal surgery: A novel neuroanatomical-based approach, (in eng). Plast Reconstr Surg Glob Open. 2016;4(12):e1181. https://doi.org/10.1097/gox.0000000000001181.
26. Singh A, Auzanneau FI, Rogers MA. Advances in edible oleogel technologies - A decade in review. Food Res Int. 2017;97:307–17. https://doi.org/10.1016/j.foodres.2017.04.022.
27. Wang Z, Chandrapala J, Truong T, Farahnaky A. Oleogels prepared with low molecular weight gelators: Texture, rheology and sensory properties, a review. Crit Rev Food Sci Nutr. 2022;1–45. https://doi.org/10.1080/10408398.2022.2027339.
28. Esposito CL, Kirilov P, Roullin VG. Organogels, promising drug delivery systems: an update of state-of-the-art and recent applications. J Control Release. 2018;271:1–20. https://doi.org/10.1016/j.jconrel.2017.12.019.
29. Hamed R, AbuRezeq A, Tarawneh O. Development of hydrogels, oleogels, and bigels as local drug delivery systems for periodontitis, (in eng). Drug Dev Ind Pharm. 2018;44(9):1488–97. https://doi.org/10.1080/03639045.2018.1464021.
30. Macoon R, Guerriero T, Chauhan A. Extended release of dexamethasone from oleogel based rods, (in eng). J Colloid Interface Sci. 2019;555:331–41. https://doi.org/10.1016/j.jcis.2019.07.082.
31. Vintiloiu A, Leroux JC. Organogels and their use in drug delivery–a review. J Control Release. 2008;125(3):179–92. https://doi.org/10.1016/j.jconrel.2007.09.014.
32. Overstreet DJ, Zdrale G, McLaren AC. Extended release of bupivacaine from temperature-responsive PNDJ hydrogels improves postoperative weight-bearing in rabbits following knee surgery. Pharmaceuticals. 2024;17(7):879. [Online]. Available: https://www.mdpi.com/1424-8247/17/7/879.
33. Wojtalewicz S, et al. Assessment of glyceride-structured oleogels as an injectable extended-release delivery system of bupivacaine, (in eng). Int J Pharm. 2023;637:122887. https://doi.org/10.1016/j.ijpharm.2023.122887.
34. Doufène K, et al. Vegetable oil-based hybrid microparticles as a green and biocompatible system for subcutaneous drug delivery, (in eng). Int J Pharm. 2021;592:120070. https://doi.org/10.1016/j.ijpharm.2020.120070.
35. Castel D, Willentz E, Doron O, Brenner O, Meilin S. Characterization of a porcine model of post-operative pain. Eur J Pain. 2014;18(4):496–505. https://doi.org/10.1002/j.1532-2149.2013.00399.x.
36. Castel D, Schauder A, Aizenberg I, Meilin S. Validation of a Gottingen Minipig model of post-operative incisional pain. J Anesth Surg Care. 2021;2:13. https://doi.org/10.17303/jasc.2020.2.10.
37. Robinson TE, Hughes EAB, Eisenstein NM, Grover LM, Cox SC. The quantification of injectability by mechanical testing. J Visualized Exp. 2020;13(159):e61417. https://doi.org/10.3791/61417.
38. Wojtalewicz S, et al. Evaluating the influence of particle morphology and density on the viscosity and injectability of a novel long-acting local anesthetic suspension. J Biomater Appl. 2022;37(4):08853282221106486. https://doi.org/10.1177/08853282221106486.
39. Robinson TE, et al. Filling the gap: A correlation between objective and subjective measures of injectability. Adv Healthc Mater. 2020;9(5):1901521. https://doi.org/10.1002/adhm.201901521.
40. Yang S, Yang G, Chen X, Chen J, Liu W. Interaction of monopalmitate and carnauba wax on the properties and crystallization behavior of soybean oleogel. Grain Oil Sci Technol. 2020;3(2):49–56. https://doi.org/10.1016/j.gaost.2020.05.001.
41. Shah JC, Maniar M. pH-Dependent solubility and dissolution of bupivacaine and its relevance to the formulation of a controlled release system. J Control Release. 1993;23(3):261–70. https://doi.org/10.1016/0168-3659(93)90007-r.
42. Manna S, et al. Probing the mechanism of bupivacaine drug release from multivesicular liposomes. J Control Release. 2019;294:279–87. https://doi.org/10.1016/j.jconrel.2018.12.029.
43. Curley J, et al. Prolonged regional nerve blockade: Injectable biodegradable bupivacaine/polyester microspheres. Anesthesiology. 1996;84(6):1401–10. https://doi.org/10.1097/00000542-199606000-00017.
44. 5-Mathematical models of drug release. In: Bruschi ML, editor. In: Strategies to modify the drug release from pharmaceutical systems. Woodhead Publishing; 2015. p. 63–86. https://doi.org/10.1016/B978-0-08-100092-2.00005-9.
45. Castel D, Willentz E, Doron O, Brenner O, Meilin S. Characterization of a porcine model of post-operative pain. Eur J Pain. 2014;18(4):496–505. https://doi.org/10.1002/j.1532-2149.2013.00399.x.
46. RettoreAndreis F, Mørch CD, Jensen W, Meijs S. On determining the mechanical nociceptive threshold in pigs: a reliability study, (in eng). Front Pain Res (Lausanne). 2023;4:1191786. https://doi.org/10.3389/fpain.2023.1191786.
47. Ison SH, Clutton RE, Di Giminiani P, Rutherford KM. A review of pain assessment in pigs, (in eng). Front Vet Sci. 2016;3:108. https://doi.org/10.3389/fvets.2016.00108.
48. Cornet S, et al. Intraoperative abobotulinumtoxinA alleviates pain after surgery and improves general wellness in a translational animal model. Sci Rep. 2022;12(1):21555. https://doi.org/10.1038/s41598-022-25002-x.
49. Pérez Fraga P, Gerencsér L, Andics A. Human proximity seeking in family pigs and dogs. Sci Rep. 2020;10(1):20883. https://doi.org/10.1038/s41598-020-77643-5.

50. Arita-Merino N, van Valenberg H, Gilbert EP, Scholten E. Quantitative phase analysis of complex fats during crystallization. Cryst Growth Des. 2020;20(8):5193–202. https://doi.org/10.1021/acs.cgd.0c00416.
51. Giannini C, Ladisa M, Altamura D, Siliqi D, Sibillano T, De Caro L. X-ray diffraction: a powerful technique for the multiple-length-scale structural analysis of nanomaterials. Crystals. 2016;6(8):87. Available: https://www.mdpi.com/2073-4352/6/8/87. Accessed July 2024.
52. von Lospichl B, et al. Injectable hydrogels for treatment of osteoarthritis – A rheological study. Colloids Surf B: Biointerfaces. 2017;159:477–83. https://doi.org/10.1016/j.colsurfb.2017.07.073.
53. Ilfeld BM, Eisenach JC, Gabriel RA. Clinical effectiveness of liposomal bupivacaine administered by infiltration or peripheral nerve block to treat postoperative pain. Anesthesiology. 2021;134(2):283–344. https://doi.org/10.1097/ALN.0000000000003630.
54. Ekelund A, Peredistijs A, Grohs J, Meisner J, Verity N, Rasmussen S. SABER-Bupivacaine Reduces Postoperative Pain and Opioid Consumption After Arthroscopic Subacromial Decompression: A Randomized, Placebo-Controlled Trial. J Am Acad Orthop Surg Glob Res Rev. 2022;6(5):e21. https://doi.org/10.5435/JAAOSGlobal-D-21-00287.
55. Le Dare B, Gicquel T. Therapeutic applications of ethanol: A review. J Pharm Pharm Sci. 2019;22(1):525–35. https://doi.org/10.18433/jpps30572.
56. Thakur RR, McMillan HL, Jones DS. Solvent induced phase inversion-based in situ forming controlled release drug delivery implants. J Control Release. 2014;176:8–23. https://doi.org/10.1016/j.jconrel.2013.12.020.
57. Larsen SW, Frost AB, Ostergaard J, Marcher H, Larsen C. On the mechanism of drug release from oil suspensions in vitro using local anesthetics as model drug compounds. Eur J Pharm Sci. 2008;34(1):37–44. https://doi.org/10.1016/j.ejps.2008.02.005.
58. Fredholt K, Larsen DH, Larsen C. Modification of in vitro drug release rate from oily parenteral depots using a formulation approach, (in eng). Eur J Pharm Sci. 2000;11(3):231–7. https://doi.org/10.1016/s0928-0987(00)00104-4.
59. Larsen DB, Parshad H, Fredholt K, Larsen C. Characteristics of drug substances in oily solutions. Drug release rate, partitioning and solubility. Int J Pharm. 2002;232(1):107–17. https://doi.org/10.1016/S0378-5173(01)00904-8.
60. Park C, Maleky F. A critical review of the last 10 years of oleogels in food. Front Sustain Food Syst. 2020;4:139. https://doi.org/10.3389/fsufs.2020.00139.
61. Davis B, et al. Entrapping bupivacaine-loaded emulsions in a crosslinked-hydrogel increases anesthetic effect and duration in a rat sciatic nerve block model. Int J Pharm. 2020;588:119703. https://doi.org/10.1016/j.ijpharm.2020.119703.
62. Adlerz KM, Aranda-Espinoza H, Hayenga HN. Substrate elasticity regulates the behavior of human monocyte-derived macrophages, (in eng). Eur Biophys J. 2016;45(4):301–9. https://doi.org/10.1007/s00249-015-1096-8.
63. Jain N, Moeller J, Vogel V. Mechanobiology of macrophages: How physical factors coregulate macrophage plasticity and phagocytosis. Annu Rev Biomed Eng. 2019;21(1):267–97. https://doi.org/10.1146/annurev-bioeng-062117-121224.
64. Ni Y, et al. Macrophages modulate stiffness-related foreign body responses through plasma membrane deformation. Proc Natl Acad Sci. 2023;120(3):e2213837120. https://doi.org/10.1073/pnas.2213837120.
65. Schwartz JB, Simonelli AP, Higuchi WI. Drug release from wax matrices I. Analysis of data with first-order kinetics and with the diffusion-controlled model. J Pharm Sci. 1968;57(2):274–7. https://doi.org/10.1002/jps.2600570206.
66. EXPAREL. Highlights of prescribing information, PACIRA. 2015. https://www.accessdata.fda.gov/drugsatfda_docs/label/2015/022496s019lbl.pdf. Accessed July 2024.
67. Sinatra R. Causes and consequences of inadequate management of acute pain. Pain Med. 2010;11(12):1859–71. https://doi.org/10.1111/j.1526-4637.2010.00983.x.
68. Kempe S, Mader K. In situ forming implants - an attractive formulation principle for parenteral depot formulations. J Control Release. 2012;161(2):668–79. https://doi.org/10.1016/j.jconrel.2012.04.016.
69. Anderson JM, Rodriguez A, Chang DT. Foreign body reaction to biomaterials, (in eng). Semin Immunol. 2008;20(2):86–100. https://doi.org/10.1016/j.smim.2007.11.004.